HHS Public Access

Author manuscript

Oncogene. Author manuscript; available in PMC 2013 February 23.

Published in final edited form as:

Oncogene. 2012 August 23; 31(34): 3889–3900. doi:10.1038/onc.2011.544.

Defining MAP3Kinases Required for MDA-MB-231 Cell Tumor Growth and Metastasis

Mark R. Cronan[1,2,4], **Kazuhiro Nakamura**[1,4], **Nancy L. Johnson**[1,4], **Deborah A. Granger**[1,4], **Bruce D. Cuevas**[5], **Jian-Guo Wang**[3,4], **Nigel Mackman**[3,4], **John E. Scott**[6], **Henrik G. Dohlman**[2,4], and **Gary L. Johnson**[1,4]

[1]Department of Pharmacology, University of North Carolina School of Medicine, Chapel Hill, NC 27599, USA

[2]Department of Biochemistry and Biophysics, University of North Carolina School of Medicine, Chapel Hill, NC 27599, USA

[3]Division of Hematology and Oncology, Department of Medicine, McAllister Heart Institute, University of North Carolina School of Medicine, Chapel Hill, NC 27599, USA

[4]Lineberger Comprehensive Cancer Center, University of North Carolina School of Medicine, Chapel Hill, NC 27599, USA

[5]Department of Molecular Pharmacology and Therapeutics, Stritch School of Medicine, Loyola University Chicago, Maywood, IL 60153 USA

[6]Department of Pharmaceutical Sciences, Biomanufacturing Research Institute and Technology Enterprise, North Carolina Central University, Durham, NC 27707, USA

Abstract

Analysis of patient tumors suggests multiple MAP3kinases (MAP3Ks) are critical for growth and metastasis of cancer cells. MAP3Ks selectively control the activation of ERK1/2, JNK, p38 and ERK5 in response to receptor tyrosine kinases and GTPases. We used MDA-MB-231 cells because of their ability to metastasize from the breast fat pad to distant lymph nodes for an orthotopic xenograft model to screen the function of seven MAP3Ks in controlling tumor growth and metastasis. Stable shRNA knockdown was used to inhibit the expression of each of the seven MAP3Ks, which were selected for their differential regulation of the MAPK network. The screen identified two MAP3Ks, MEKK2 and MLK3, whose shRNA knockdown caused significant inhibition of both tumor growth and metastasis. Neither MEKK2 nor MLK3 have been previously shown to regulate tumor growth and metastasis *in vivo*. These results demonstrated that MAP3Ks, which differentially activate JNK, p38 and ERK5 are necessary for xenograft tumor growth and metastasis of MDA-MB-231 tumors. The requirement for MAP3Ks signaling through multiple MAPK pathways explains why several members of the MAPK network are activated in cancer.

Corresponding author: Gary L. Johnson, Department of Pharmacology, University of North Carolina at Chapel Hill, Chapel Hill, NC 27599-7365, glj@med.unc.edu, Phone: (919) 843-3107, Fax: (919) 966-5640.

Conflict of interest

The authors declare no conflict of interest.

MEKK2 was required for EGF receptor and Her2/Neu activation of ERK5, with ERK5 being required for metastasis. Loss of MLK3 expression increased mitotic infidelity and apoptosis *in vitro*. Knockdown of MEKK2 and MLK3 resulted in increased apoptosis in orthotopic xenografts relative to control tumors in mice, inhibiting both tumor growth and metastasis; MEKK2 and MLK3 represent untargeted kinases in tumor biology for potential therapeutic development.

Keywords

MAP3K; Metastasis; MAPK network; MEKK2; MLK3

Introduction

In mammalian cells, 22 defined MAP3Ks, 11 MAP2Ks and 7 MAPKs comprise a signaling network involving at least 40 protein kinases (Cuevas et al 2007). The MAPK network represents approximately 8% of the human kinome and as such it is not surprising that members of the MAPK signaling network are frequently amplified, overexpressed and activated in cancer (Wagner and Nebreda 2009). Elevated expression and/or activation of JNK, p38 and ERK5 has been demonstrated in many cancers including breast, prostate, squamous and hepatocellular carcinoma and generally correlate with poor survival (Davidson et al 2006, Hui et al 2008, McCracken et al 2008, Sticht et al 2008, Wang et al 2010, Zen et al 2009, Montero et al 2009). Thus, despite the prominent role of the Ras-Raf-MEK1/2-ERK1/2 pathway in cancer, patient tumor analysis suggests other kinases within the MAPK network are critical for growth and metastasis of cancer cells.

Activation of the ERK1/2, JNK, p38 and ERK5 MAPKs is controlled by upstream MAP3Ks that are frequently dysregulated in cancer cells. Activating mutations of B-Raf are found in ~7% of all tumors and about 60% of melanomas, resulting in constitutive activation of ERK1/2 (Davies et al 2002). In these tumors, activating B-Raf mutations correlate with poor survival, recurrence and resistance to chemotherapy (Samowitz et al 2005, Sheridan et al 2008). The MAP3K Tpl2 has been shown to be amplified and overexpressed in 40% of human breast cancers (Sourvinos et al 1999). A predicted activating Tpl2 mutation was also found in a patient with primary basal-like breast cancer and cells containing this Tpl2 mutation were preferentially enriched in a metastasis from the primary tumor (Ding et al 2010). The MAP3Ks MEKK3 and A-Raf were found recently to be overexpressed in non-small cell lung cancer (Lee et al 2010).

Despite the overwhelming evidence from the analysis of patient tumor samples that the MAPK signaling network is significantly dysregulated in cancer, there is little definitive understanding of the actual function of MAP3K signaling in regulating tumor growth and metastasis. The exception is the MAP3Ks, B-Raf and c-Raf, which enhance cell proliferation through ERK1/2 signaling (Davies et al 2002). Most MAP3Ks regulate at least two different MAPKs such as JNK and p38 (e.g., MLK3) or ERK5 and JNK (e.g., MEKK2) (Brancho et al 2005, Cuevas et al 2007, Kesavan et al 2004). Thus, the MAPK signaling network should be viewed not simply as multiple independent pathways but as a cooperative

network involving many MAP3Ks that dynamically integrate different cellular stimuli to coordinately activate downstream MAPKs.

In this study, we used the triple negative MDA-MB-231 claudin-low breast cancer line to assess seven MAP3Ks for their role in tumor growth and metastasis through selective shRNA knockdown using orthotopic breast fat pad xenografts (Prat et al 2010). The orthotopic xenograft screen was done with MDA-MB-231 cells because they are the only line we tested that gave significant metastasis to distant lymph nodes; this was not true for other lines tested including SUM149, SUM159, Hs578T and BT474 cells. Our goal was to identify MAP3Ks whose loss of expression could inhibit metastasis in addition to tumor growth. We analyzed seven MAP3Ks expressed in MDA-MB-231 cells representing a cross section of the MAP3Ks that differentially regulate ERK1/2, JNK, p38 and ERK5. Except for B-Raf, MAP3Ks chosen for study represent “untargeted kinases” in that they are generally poorly characterized in disease models including cancer. The findings identified two MAP3Ks previously untargeted in cancer that were required for tumor growth and metastasis of MDA-MB-231 cells.

Results

MAP3Ks control tumor growth and metastasis

We set out to test the role of specific MAP3Ks in tumor growth and metastasis using MDA-MB-231 cells. To start, we used siRNA knockdown of kinases in the MAPK network and measured cell proliferation and possible synthetic lethal phenotypes in the presence of MEK1/2, JNK or p38 inhibitors (Supplementary Figure S1A–C). The screen showed growth of MDA-MB-231 cells in culture was dependent on expression of ERK2 (MAPK1) and partially on the upstream MAP3K B-Raf. Knockdown of other kinases in the network did not significantly inhibit proliferation in the presence or absence of inhibitors, even though JNK small molecule inhibitor strongly inhibited growth of the cells similar to that seen with MEK1/2 inhibitor (Supplementary Figure S1D). It was decided that such *in vitro* assays were inadequate and a more functional assay was needed to test the role of MAP3Ks, for example those activating JNK or ERK5, for control of MDA-MB-231 tumorigenesis. We therefore chose to use stable shRNA knockdown in MDA-MB-231 cells and orthotopic breast fat pad xenografts to test the function of specific MAP3Ks. Seven MAP3Ks expressed in MDA-MB-231 cells that differentially regulate ERK1/2, JNK, p38 and ERK5 were selected for stable shRNA knockdown for analysis in orthotopic xenografts.

Figure 1a shows the seven MAP3Ks and their regulation of downstream MAPKs chosen for shRNA knockdown. The MAP3Ks selected for shRNA knockdown signal through ERK1/2 (B-Raf and Tpl2), ERK1/2 and JNK (MEKK1), JNK and p38 (TAK1, MLK3), JNK and ERK5 (MEKK2) or p38 and ERK5 (MEKK3). In general, two or more shRNAs were used for creating independent knockdown lines for each MAP3K. Ultrasound and bioluminescent imaging (BLI) enabled longitudinal tracking of tumor growth and metastasis of cells having shRNA knockdown of MAP3Ks (Figure 1b). Knockdown of each kinase was assessed by either western blotting or real-time PCR in the cells before implantation in the mammary fat pad and in metastases after animal sacrifice at 6–8 weeks post tumor initiation (Supplementary Figure S2A-L).

MEKK1—We have previously shown that RNAi-mediated loss of MEKK1 expression in MDA-MB-231 cells resulted in significant inhibition of both cell migration and invasion through Matrigel (Cuevas et al 2006). Mammary fat pad orthotopic xenografts of MDA-MB-231 cells having knockdown of MEKK1 formed tumors similar to wild type cells but failed to metastasize to lymph nodes during a 12 week longitudinal study (Figure 1c and d). In contrast, four mice having wild-type MDA-MB-231 cells injected into mammary fat pads each developed metastases. The results with MDA-MB-231 orthotopic xenografts were similar to our studies with the MMTV-PyMT mouse breast cancer model, where mammary tumors developed metastases and targeted deletion of MEKK1 significantly delayed breast cancer metastasis while tumor growth was unchanged (Cuevas et al 2006). The significant delay of metastasis was due in part to a loss of urokinase type-1 plasminogen activator (uPA) expression, which is also seen in MDA-MB-231 cells having RNAi knockdown of MEKK1 (Cuevas et al 2006). Similar *in vivo* phenotypes with shRNA knockdown of MEKK1 in MDA-MB-231 cells implanted in the mammary fat pad and targeted deletion of MEKK1 in the MMTV-PyMT mouse validated MDA-MB-231 orthotopic xenografts as a model to assess MAP3K signaling in controlling metastasis. We therefore used this orthotopic xenograft assay to screen functional consequences of shRNA knockdown of six additional MAP3Ks in MDA-MB-231 cells. The goal was to discover understudied MAP3Ks required for tumor growth and metastasis.

B-Raf and Tpl2—B-Raf and Tpl2 each regulate ERK1/2 activity. Similar to the siRNA screen (Supplementary Figure S1), stable shRNA knockdown of B-Raf resulted in decreased MDA-MB-231 cell growth and ERK1/2 activity in cultured cells (Figure 2a-d). In knockdown xenografts, with 90% loss of B-Raf protein expression (Supplementary Figure S2A), tumors were still able to implant but were significantly smaller in size, consistent with decreased tumor cell proliferation (Figure 2e and g). Tumors having B-Raf knockdown formed metastases at what appeared to be a somewhat lower frequency than control cells (Figure 2f and h). However, with a total of 13 and 12 mice with control and B-Raf knockdown tumors, respectively, the difference in number of metastases was not statistically significant (p_{pooled}=0.23). At seven-eight weeks post tumor implant the bioluminescent photon flux measurements of metastases from B-Raf knockdown tumors was less compared to control tumors, consistent with inhibited proliferation with B-Raf knockdown (Supplementary Table S1).

Tpl2 knockdown, like B-Raf, also had an inhibitory effect on xenograft tumor growth (Figure 3a–b), even though Tpl2 knockdown did not inhibit cell growth *in vitro* (Supplementary Figure S1). Six of fifteen mice with Tpl2 knockdown tumors formed metastases compared to five of eight mice with tumors from control cells (Figure 3a–c), which was not statistically significantly different for the two conditions (p_{pooled}=0.40). Bioluminescent photon flux measurements of metastases from Tpl2 knockdown tumors were less compared to control tumors, similar to that observed with B-Raf (Supplementary Table S1). Thus, both B-Raf and Tpl2 knockdown inhibited tumor cell growth *in vivo*, consistent with both MAP3Ks playing a critical role in controlling proliferation.

MEKK3 and TAK1—MEKK3 binds the scaffold protein p62/sequestosome 1 and localizes in cytosolic aggregates or speckles for the control of NFκB (Nakamura et al 2010). MEKK3 also regulates JNK and ERK5 independent of p62/sequestosome 1. Similar to B-Raf and Tpl2, knockdown of MEKK3 inhibited tumor growth but did not change the frequency of metastasis (Figure 3d–f).

Knockdown of TAK1, which also regulates JNK and p38, had no effect on tumor growth or the frequency of metastases (Figure 3g–i). Only one shRNA is shown for TAK1 because other shRNAs did not sustain knockdown over a seven week longitudinal study in mice (Supplementary Figure S2 and data not shown). The fact that metastases retained TAK1 knockdown with shRNA1 indicated TAK1 is not essential for metastases.

MEKK2—MEKK2 regulates ERK5 activation in response to growth factor receptor tyrosine kinases (Kesavan et al 2004, Sun et al 2003). MEKK2 immunoprecipitation identified EGFR as a co-immunoprecipitating protein (data not shown), indicating MEKK2 and EGFR are in a signaling complex in cells. We found MEKK2 knockdown inhibits activation of ERK5 in response to EGF in MDA-MB-231 cells (Figure 4a), as well as SUM159 and Hs578T cells (Supplementary Figure S3A–B). In contrast to ERK5 signaling, ERK1/2 and JNK1 activation was unchanged. Previous studies suggested that MEKK2 activates ERK5 in a Src dependent manner (Sun et al 2003), so we tested if Src was required for EGF stimulated ERK5 activation using the Src inhibitors PP2 and Dasatinib, the inactive inhibitor PP3 and the highly selective EGFR/Her2 inhibitor Lapatinib. EGFR phosphorylation and ERK5 activation was dependent on EGFR kinase activity and MEKK2-dependent ERK5 activation is enhanced but not dependent on Src (Figure 4b).

Overexpression of the EGFR family member Her2/Neu in BT474 cells constitutively activates ERK5 (Montero et al 2009). MEKK2 knockdown blocked constitutive activation of ERK5 in BT474 cells (Figure 4c). While ERK5 was predominantly in the activated, gel shifted state in control cells, ERK5 was in the inactive, dephosphorylated form in MEKK2 shRNA knockdown cells. This was accompanied by an increase in JNK phosphorylation, whereas ERK1/2 activation remained unchanged.

shRNA knockdown of MEKK2 strongly inhibited both tumor growth and metastasis (Figure 4d–g). Knockdown of MEKK2 showed diminished tumor growth, resulting in tumors that were ~10–33% the size of control tumors. Metastasis was detected in only one of 12 mice from MEKK2 shRNA knockdown tumors versus 7 of 13 mice injected with control cells (Figure 4e and g), giving a highly significant inhibition of measureable metastases (p_{pooled}=0.0155). The small tumor size allowed mice harboring MEKK2 knockdown tumors to be maintained in a healthy state for longer times to monitor metastasis. Metastasis was delayed greater than five weeks (7 weeks in controls vs. >12 weeks in MEKK2 shRNA tumors) with MEKK2 shRNA tumors; with the metastases retaining knockdown of MEKK2 during the duration of the experiment (Supplementary Figure S2K). These results were confirmed in a second set of animals (Supplementary Figure S3C and D), with the difference in number of metastases being highly significant between control and MEKK2 knockdown tumors (p_{pooled}=0.0094). Increased apoptosis assayed by TUNEL was observed with loss of MEKK2 expression in xenografts versus size matched control tumors (Supplementary

Figure S3E), although growth of MEKK2 knockdown cells in culture was the same as wild-type cells (Supplementary Figure S3F).

Tumor growth of MEKK2 shRNA knockdown BT474 cell xenografts was also inhibited (Figure 4h). BLI analysis showed a 12-fold decrease in photon flux in MEKK2 shRNA tumors relative to control (Figure 4i). Thus, MEKK2 is critical for EGF receptor and Her2/Neu tyrosine kinase-dependent ERK5 activation, tumor growth of both MDA-MB-231 and BT474 cells, and metastasis of MDA-MB-231 cells.

ERK5 knockdown inhibits metastasis—Because MEKK2 is required for EGF receptor activation of ERK5, we next assessed whether knockdown of ERK5 in MDA-MB-231 cells would show similar tumor growth and metastasis phenotypes as with MEKK2 knockdown. Two different shRNAs were used to inhibit ERK5 expression (Figure 5a). ERK5 knockdown resulted in a decrease in metastasis without a significant effect on tumor growth (Figure 5b and c). Only one of 10 animals injected with ERK5 shRNA knockdown cells had lymph node metastasis. Thus, MEKK2 regulation of ERK5 is only one arm of MEKK2 signaling controlling tumor growth and metastasis.

Inhibition of tissue factor associated microparticle release in MEKK2 knockdown cells—Growth of MEKK2 knockdown cells was normal *in vitro*, indicating the MEKK2-MEK5-ERK5 pathway is not required for proliferation in culture (Supplementary Figure S3F). This contrasts with the inhibition of xenograft tumor growth and metastasis, so we screened for secreted factors including proteases and cytokines that could affect xenograft tumor properties (Table S2). We screened for 88 secreted analytes (http://www.rulesbasedmedicine.com/products-services/humanmap-services/humanmap/) using control, MEKK2 and MLK3 shRNA knockdown MDA-MB-231 cells. Of the 88 analytes tested only tissue factor (TF) was significantly reduced in the culture supernatants from the MEKK2 knockdown cells compared to wild-type cells (Figure 5d). A reduced level of TF in the culture supernatant was confirmed using a TF ELISA (Figure 5e). Importantly, levels of cellular TF activity were similar in MEKK2 shRNA cells and control cells (Figure 5f). TF is a transmembrane receptor that is released from the plasma membrane of tumors cells in the form of microparticles (MPs), so-called TF+ MPs that are constitutively released from tumor cells (Kasthuri et al 2009, Rak 2010). We showed the released TF was in the form of MPs by isolating MPs from the culture supernatant and measuring the level of TF activity (Khorana et al 2008). We found a significant reduction on TF+ MPs in the culture supernatant from MEKK2 shRNA cells compared to controls (Figure 5g). Diminished release of TF could also be detected by western blotting of supernatants from MDA-MB-231 cells having either stable shRNA knockdown or transient knockdown of MEKK2 with multiple siRNAs (Figure 5h–i), demonstrating the on-target effect of MEKK2 knockdown on the release of TF+ MPs from MDA-MB-231 cells. Interestingly, we could not demonstrate that knockdown of ERK5 or inhibition of JNK blocked TF+ MP release from MDA-MB-231 cells (data not shown), suggesting that MEKK2 is part of a signaling complex controlling MP formation and/or release independent of ERK5 or JNK signaling. There was no difference in released TF in the culture supernatants from MLK3 knockdown MDA-MB-231 cells (data not shown). Previous studies have shown that activated Ras and

EGF receptor signaling enhance MP release that contributes to coagulopathy and tumor angiogenesis (Al-Nedawi et al 2008, Kasthuri et al 2009, Rak 2010, Yu et al 2005). Thus, MEKK2 is an important member of an EGF receptor signaling complex controlling cancer cell TF+ MP release that is critical for tumor growth and metastasis.

MLK3—MLK3 expression is required for p38 activation in response to TGFβ and for JNK activation in response to fatty acids (Figure 6a and b) (Jaeschke and Davis 2007, Kim et al 2004). Stable MLK3 knockdown by shRNA decreased *in vitro* proliferation of MDA-MB-231, SUM159 and Hs578T cells (Figure 6c and Supplementary Figures S4A and B). This growth inhibition was greater than was observed in the transient siRNA screen over a 4 day period. There was an increase in apoptosis in MLK3 knockdown cells as determined by the percentage of cells with sub G_0/G_1 DNA content (Figure 6d and e). TUNEL staining showed increased fragmented DNA in MLK3 knockdown cells, confirming loss of MLK3 resulted in increased apoptosis (Figure 6f). MLK3 has been implicated in controlling microtubule organization with inhibition of MLK3 resulting in aberrant spindle pole formation in HeLa cells that can result in chromosomal instability (Cha et al 2006, Fodde et al 2001). We found an increase in multinucleated and micronucleated cells with MLK3 knockdown, consistent with MLK3 deficiency inducing mitotic infidelity in MDA-MB-231 cells (Figure 6g and h).

shRNA knockdown of MLK3 had a pronounced inhibition of tumor growth in mice (Figure 6i and k). The tumors remained very small over time with little evidence of continued tumor expansion. TUNEL assay for apoptotic cells in size matched MLK3 knockdown and control xenografts showed a significant increase in apoptosis in the tumors having loss of MLK3 expression (Supplementary Figure S4F), consistent with the increased apoptosis observed in culture. Loss of MLK3 expression also strongly inhibited tumor metastasis (Figure 6j and l). Because of the dramatic xenograft phenotype, we tested a third shRNA targeting MLK3, which demonstrated a similarly pronounced inhibition of tumor growth and metastasis (Figure 6m and Supplementary Figure S4C). Only a single mouse out of 32 mice injected with MLK3 shRNA cell lines developed a lymph node metastasis, while 12 of 22 mice were positive for metastasis from control MDA-MB-231 cell tumors. Similar results were observed when the MLK3 shRNA cell lines were injected into the flank rather than the fat pad (Supplementary Figure S4D and E), indicating MLK3 knockdown strongly inhibited MDA-MB-231 cell tumor growth independent of the tumor microenvironment. Thus, loss of MLK3 expression markedly inhibited both tumor growth and metastasis giving the most dramatic phenotype of the seven MAP3K knockdowns tested in the orthotopic xenograft assay.

Discussion

The orthotopic xenograft screen of MDA-MB-231 cells proved insightful and led to the discovery of two kinases not previously defined to regulate tumor growth and metastasis. Six of the seven MAP3Ks tested had some regulatory function in controlling tumor growth and/or metastasis, showing that a collective group of MAP3Ks contribute to driving the tumor phenotype. Evident in our data is the separation of tumor size and the ability to metastasize (i.e., B-Raf, Tpl2, MEKK3). This is consistent with previous observations that

small tumors may readily metastasize and large tumors may not metastasize (Husemann et al 2008, Sidebottom 1983, Wo 2011). Our findings uniquely defined MEKK2 and MLK3 as regulating both tumor growth and metastasis. The findings explain why multiple members of the MAPK network are overexpressed and/or activated in many cancers, so as to coordinately activate ERK1/2, JNK, p38 and ERK5. Loss of individual MAP3Ks by shRNA knockdown can significantly compromise the network such that tumor growth and/or metastasis are inhibited. If one uses a stringent criteria that both tumor growth and metastasis must be inhibited only MEKK2 and MLK3 of the MAP3Ks tested would be considered potential new therapeutic targets. Targeting MLK3 inhibition warrants particular focus because its loss of expression induced apoptosis while strongly inhibiting tumor growth and metastasis, both important criterion for regression of the primary tumor and prevention of metastatic spread.

The involvement of MEKK2 in cancer is not limited to breast cancer; a recent study has linked MEKK2 to prostate cancer. MEKK2 was expressed at 4.4-fold higher level in prostate cancer tissue versus benign tissue and even higher levels of MEKK2 expression were observed in LNCaP, Du145 and PC3 prostate cell lines (Cazares et al 2009). Overexpression of ERK5 and MEK5 has also been demonstrated to be important prognostic factors in prostate cancer (McCracken et al 2008, Mehta et al 2003). While inhibitors of ERK5 signaling have been characterized to inhibit the growth of specific tumors (Yang et al 2010), our findings suggest that inhibition of MEKK2 would have greater clinical benefit than inhibiting ERK5 alone because of the diverse biological role of MEKK2 in control of ERK5, JNK, and TF+ MP release (Tatake et al 2008, Yang et al 2010). In MDA-MB-231 cells ERK5 does not appear to regulate proliferation but is involved in controlling metastasis, consistent with the analysis of cancer patient data and outcome (Mehta et al 2003, Montero et al 2009).

While MLK3 has previously been characterized as pro-apoptotic in neurons (Mishra et al 2007), we find that MLK3 is anti-apoptotic in tumor cells. Inducible expression of active MLK3 in MCF10A cells grown in 3D Matrigel enhanced migration and inhibited apoptosis (Chen et al 2010), consistent with inhibition of growth and increased apoptosis in MDA-MB-231 cells having shRNA-mediated MLK3 knockdown. MLK3-dependent proliferation also has been demonstrated in K-Ras mutant pancreatic cancer cell lines using siRNA knockdown of MLK3 or MLK3 small molecule inhibitors (Chandana et al 2010). Mitotic infidelity and increased apoptosis induced by loss of MLK3 expression previously was also shown *in vitro* with a small molecule MLK3 inhibitor with cell lines having activated Ras (Cha et al 2006). Thus, MLK3 inhibition might serve as a therapeutic target worth investigating for Ras mutant tumors, which are difficult to treat and generally lack molecularly targeted therapies.

MEKK2 and MLK3 are kinases within the untargeted cancer kinome (Fedorov et al 2010). Knockdown of MEKK2 and MLK3 inhibited tumor growth to similar or greater extents as knockdown of B-Raf or Tpl-2, but also inhibited metastasis more significantly than B-Raf. Our study predicts that inhibiting MEKK2 and/or MLK3 alone or in combination with B-Raf or MEK1/2 inhibition could have significant benefit in activated Ras or B-Raf driven tumors. Previous studies have demonstrated that MLK3 and MEKK2 knockout mice are

viable and grossly normal (Brancho et al 2005, Guo et al 2002). Also, small molecule MLK3 inhibitors were well tolerated in trials for protection against neurodegeneration (Waldmeier et al 2006), suggesting that inhibitors for both MEKK2 and MLK3 would likely be well tolerated. Our results show that although labor intensive, orthotopic xenografts using shRNA knockdown of specific kinases, such as MEKK2 and MLK3, can be an effective method to define the function of untargeted and understudied kinases in cancer.

Materials and Methods

Reagents and Cell culture

TGF-β1 and EGF were from Peprotech. U0126, SP600125, SB203580, Dasatinib and Lapatinib were from LC Labs. Cell culture reagents were from Invitrogen. All other reagents were from Sigma. For bioluminescent imaging, cells were infected with luciferase expressing retroviruses and selected on G418. MDA-MB-231 and Hs578t cells were maintained in DMEM/10% FBS with 1% penicillin/streptomycin. SUM159 cells were maintained in F12 media supplemented with 5% FBS, 5 ug/mL human recombinant insulin (Gibco), 1 ug/mL hydrocortisone (Sigma) and 1% penicillin/streptomycin. BT474 cells were maintained in DMEM:F12 (1:1) containing 10% FBS and 1% penicillin/streptomycin. Cell lines used in this study were authenticated using short tandem repeat (STR) profiling.

Knockdown of MAP3Ks in cell lines

Open Biosystems TRCN shRNAs were cotransfected into HEK293 cells with pMD2.G and psPAX2 (Addgene plasmid 12259 and 12260, Trono lab) to produce lentiviral shRNA particles. Lentiviruses containing shRNAs were infected into target cells and were selected with 2 μg/mL puromycin (Clontech). TRCN clone numbers are indicated in Figure S2. For ERK5, TRCN0000001356 and TRCN0000010262 were used to knockdown ERK5.

Tumor Xenografts

Mouse experiments were performed in accordance with the UNC Institutional Care and Use Committee and NIH guidelines. Tumor xenografts were established by injecting either 2×10^6 MDA-MB-231 cells or 4×10^6 BT474 cells in a 50:50 mix of SFM:matrigel into the inguinal fat pad or flank of 8 week old SCID mice. For BT474 cells estrogen pellets were used as in Sartorius et al 2003. In general, eight mice were used for control and each shRNA knockout line per experiment.

Tumor and metastasis measurements

Tumor size was measured by calipers or ultrasound imaging using a Vevo 770 (Visualsonics). Tumor volume was calculated using the equation Volume = Length × ($\text{Width}^2/2$). Metastasis was measured by injecting mice with 100 μL of luciferin (50 mg/mL, Gold Biosciences) and imaging mice using a Xenogen IVIS 100 (Caliper Lifesciences). Images of metastases from control and shRNA cell lines were captured under identical imaging conditions at identical times after luciferin injection. Statistical significance of metastases was calculated by Fisher's exact test using Prism (GraphPad Software). Bioluminescent photon flux was measured in tumors and metastases using Living Image software (Caliper Lifesciences).

Cell Viability Assays

For each shRNA condition 1×10^3 MDA-MB-231 cells, 0.5×10^3 SUM159 cells or 2×10^3 Hs578t cells were plated in quadruplicate in 96-well plates. Drugs were added 18 hours after plating. On each day, one plate was assayed using CellTiter-Glo reagent (Promega) according to the manufacturer's protocol. Luminescence was measured on a Pherastar microplate reader (BMG Labtech) and normalized to day 0 values.

Realtime PCR of RNA Levels

Total cell line RNA was extracted with the RNeasy kit (Qiagen). 3μg total RNA was reverse transcribed using the High Capacity cDNA Reverse Transcription kit (Applied Biosystems). Realtime PCR was performed with Taqman gene expression assays (Applied Biosystems) on an Applied Biosystems 7500 Fast real-time PCR system by 3 step denaturing, annealing and elongation process. Results for all targets were normalized to human β-actin message.

siRNA screening of MAPK genes, m*easurement of Tissue Factor antigen and activity*, *western blotting*, p*ropidium iodide staining and immunofluorescence.* See supplementary methods.

Supplementary Material

Refer to Web version on PubMed Central for supplementary material.

Acknowledgments

This work was supported by NIH grants GM30324 (GLJ), DK37871 (GLJ), GM059167 (HGD), U54CA156735 (GLJ and JES) and CA120881 (BC) and the University of North Carolina Cancer Research Fund (GLJ). We acknowledge the RNAi Screening Core and Lentiviral shRNA Core for support of this research.

References

Al-Nedawi K, Meehan B, Micallef J, Lhotak V, May L, Guha A, et al. Intercellular transfer of the oncogenic receptor EGFRvIII by microvesicles derived from tumour cells. Nat Cell Biol. 2008; 10:619–624. [PubMed: 18425114]

Brancho D, Ventura JJ, Jaeschke A, Doran B, Flavell RA, Davis RJ. Role of MLK3 in the regulation of mitogen-activated protein kinase signaling cascades. Mol Cell Biol. 2005; 25:3670–3681. [PubMed: 15831472]

Cazares LH, Troyer D, Mendrinos S, Lance RA, Nyalwidhe JO, Beydoun HA, et al. Imaging mass spectrometry of a specific fragment of mitogen-activated protein kinase/extracellular signal-regulated kinase kinase kinase 2 discriminates cancer from uninvolved prostate tissue. Clin Cancer Res. 2009; 15:5541–5551. [PubMed: 19690195]

Cha H, Dangi S, Machamer CE, Shapiro P. Inhibition of mixed-lineage kinase (MLK) activity during G2-phase disrupts microtubule formation and mitotic progression in HeLa cells. Cell Signal. 2006; 18:93–104. [PubMed: 15923109]

Chandana SR, Leece CM, Gallo KA, Madhukar BV, Conley BA. Inhibition of MLK3 Decreases Proliferation and Increases Antiproliferative Activity of Epidermal Growth Factor Receptor (EGFR) Inhibitor in Pancreatic Cancer Cell Lines. Cancer Growth and Metastasis. 2010; 2010:1.

Chen J, Miller EM, Gallo KA. MLK3 is critical for breast cancer cell migration and promotes a malignant phenotype in mammary epithelial cells. Oncogene. 2010; 29:4399–4411. [PubMed: 20514022]

Cuevas BD, Winter-Vann AM, Johnson NL, Johnson GL. MEKK1 controls matrix degradation and tumor cell dissemination during metastasis of polyoma middle-T driven mammary cancer. Oncogene. 2006; 25:4998–5010. [PubMed: 16568086]

Cuevas BD, Abell AN, Johnson GL. Role of mitogen-activated protein kinase kinase kinases in signal integration. Oncogene. 2007; 26:3159–3171. [PubMed: 17496913]

Davidson B, Konstantinovsky S, Kleinberg L, Nguyen MT, Bassarova A, Kvalheim G, et al. The mitogen-activated protein kinases (MAPK) p38 and JNK are markers of tumor progression in breast carcinoma. Gynecol Oncol. 2006; 102:453–461. [PubMed: 16494928]

Davies H, Bignell GR, Cox C, Stephens P, Edkins S, Clegg S, et al. Mutations of the BRAF gene in human cancer. Nature. 2002; 417:949–954. [PubMed: 12068308]

Ding L, Ellis MJ, Li S, Larson DE, Chen K, Wallis JW, et al. Genome remodelling in a basal-like breast cancer metastasis and xenograft. Nature. 2010; 464:999–1005. [PubMed: 20393555]

Fedorov O, Muller S, Knapp S. The (un)targeted cancer kinome. Nat Chem Biol. 2010; 6:166–169. [PubMed: 20154661]

Fodde R, Kuipers J, Rosenberg C, Smits R, Kielman M, Gaspar C, et al. Mutations in the APC tumour suppressor gene cause chromosomal instability. Nat Cell Biol. 2001; 3:433–438. [PubMed: 11283620]

Gjerdrum C, Tiron C, Hoiby T, Stefansson I, Haugen H, Sandal T, et al. Axl is an essential epithelial-to-mesenchymal transition-induced regulator of breast cancer metastasis and patient survival. Proc Natl Acad Sci U S A. 2010; 107:1124–1129. [PubMed: 20080645]

Guo Z, Clydesdale G, Cheng J, Kim K, Gan L, McConkey DJ, et al. Disruption of Mekk2 in mice reveals an unexpected role for MEKK2 in modulating T-cell receptor signal transduction. Mol Cell Biol. 2002; 22:5761–5768. [PubMed: 12138187]

Hui L, Zatloukal K, Scheuch H, Stepniak E, Wagner EF. Proliferation of human HCC cells and chemically induced mouse liver cancers requires JNK1-dependent p21 downregulation. J Clin Invest. 2008; 118:3943–3953. [PubMed: 19033664]

Husemann Y, Geigl JB, Schubert F, Musiani P, Meyer M, Burghart E, et al. Systemic spread is an early step in breast cancer. Cancer Cell. 2008; 13:58–68. [PubMed: 18167340]

Jaeschke A, Davis RJ. Metabolic stress signaling mediated by mixed-lineage kinases. Mol Cell. 2007; 27:498–508. [PubMed: 17679097]

Kasthuri RS, Taubman MB, Mackman N. Role of tissue factor in cancer. J Clin Oncol. 2009; 27:4834–4838. [PubMed: 19738116]

Kesavan K, Lobel-Rice K, Sun W, Lapadat R, Webb S, Johnson GL, et al. MEKK2 regulates the coordinate activation of ERK5 and JNK in response to FGF-2 in fibroblasts. J Cell Physiol. 2004; 199:140–148. [PubMed: 14978743]

Khorana AA, Francis CW, Menzies KE, Wang JG, Hyrien O, Hathcock J, et al. Plasma tissue factor may be predictive of venous thromboembolism in pancreatic cancer. J Thromb Haemost. 2008; 6:1983–1985. [PubMed: 18795992]

Kim KY, Kim BC, Xu Z, Kim SJ. Mixed lineage kinase 3 (MLK3)-activated p38 MAP kinase mediates transforming growth factor-beta-induced apoptosis in hepatoma cells. J Biol Chem. 2004; 279:29478–29484. [PubMed: 15069087]

Lee W, Jiang Z, Liu J, Haverty PM, Guan Y, Stinson J, et al. The mutation spectrum revealed by paired genome sequences from a lung cancer patient. Nature. 2010; 465:473–477. [PubMed: 20505728]

McCracken SR, Ramsay A, Heer R, Mathers ME, Jenkins BL, Edwards J, et al. Aberrant expression of extracellular signal-regulated kinase 5 in human prostate cancer. Oncogene. 2008; 27:2978–2988. [PubMed: 18071319]

Mehta PB, Jenkins BL, McCarthy L, Thilak L, Robson CN, Neal DE, et al. MEK5 overexpression is associated with metastatic prostate cancer, and stimulates proliferation, MMP-9 expression and invasion. Oncogene. 2003; 22:1381–1389. [PubMed: 12618764]

Mishra R, Barthwal MK, Sondarva G, Rana B, Wong L, Chatterjee M, et al. Glycogen synthase kinase-3beta induces neuronal cell death via direct phosphorylation of mixed lineage kinase 3. J Biol Chem. 2007; 282:30393–30405. [PubMed: 17711861]

Montero JC, Ocana A, Abad M, Ortiz-Ruiz MJ, Pandiella A, Esparis-Ogando A. Expression of Erk5 in early stage breast cancer and association with disease free survival identifies this kinase as a potential therapeutic target. PLoS One. 2009; 4:e5565. [PubMed: 19440538]

Nakamura K, Kimple AJ, Siderovski DP, Johnson GL. PB1 domain interaction of p62/sequestosome 1 and MEKK3 regulates NF-kappaB activation. J Biol Chem. 2010; 285:2077–2089. [PubMed: 19903815]

Pao-Chun L, Chan PM, Chan W, Manser E. Cytoplasmic ACK1 interaction with multiple receptor tyrosine kinases is mediated by Grb2: an analysis of ACK1 effects on Axl signaling. J Biol Chem. 2009; 284:34954–34963. [PubMed: 19815557]

Prat A, Parker JS, Karginova O, Fan C, Livasy C, Herschkowitz JI, et al. Phenotypic and molecular characterization of the claudin-low intrinsic subtype of breast cancer. Breast Cancer Res. 2010; 12:R68. [PubMed: 20813035]

Rak J. Microparticles in cancer. Semin Thromb Hemost. 2010; 36:888–906. [PubMed: 21049390]

Samowitz WS, Sweeney C, Herrick J, Albertsen H, Levin TR, Murtaugh MA, et al. Poor survival associated with the BRAF V600E mutation in microsatellite-stable colon cancers. Cancer Res. 2005; 65:6063–6069. [PubMed: 16024606]

Sartorius CA, Shen T, Horwitz KB. Progesterone receptors A and B differentially affect the growth of estrogen-dependent human breast tumor xenografts. Breast Cancer Res Treat. 2003; 79:287–299. [PubMed: 12846413]

Sheridan C, Brumatti G, Martin SJ. Oncogenic B-RafV600E inhibits apoptosis and promotes ERK-dependent inactivation of Bad and Bim. J Biol Chem. 2008; 283:22128–22135. [PubMed: 18508762]

Sidebottom E, Clark SR. Cell fusion segregates progressive growth from metastasis. Br J Cancer. 1983; 47:399–406. [PubMed: 6830690]

Sourvinos G, Tsatsanis C, Spandidos DA. Overexpression of the Tpl-2/Cot oncogene in human breast cancer. Oncogene. 1999; 18:4968–4973. [PubMed: 10490831]

Sticht C, Freier K, Knopfle K, Flechtenmacher C, Pungs S, Hofele C, et al. Activation of MAP kinase signaling through ERK5 but not ERK1 expression is associated with lymph node metastases in oral squamous cell carcinoma (OSCC). Neoplasia. 2008; 10:462–470. [PubMed: 18472963]

Sun W, Wei X, Kesavan K, Garrington TP, Fan R, Mei J, et al. MEK kinase 2 and the adaptor protein Lad regulate extracellular signal-regulated kinase 5 activation by epidermal growth factor via Src. Mol Cell Biol. 2003; 23:2298–2308. [PubMed: 12640115]

Tatake RJ, O'Neill MM, Kennedy CA, Wayne AL, Jakes S, Wu D, et al. Identification of pharmacological inhibitors of the MEK5/ERK5 pathway. Biochem Biophys Res Commun. 2008; 377:120–125. [PubMed: 18834865]

Wagner EF, Nebreda AR. Signal integration by JNK and p38 MAPK pathways in cancer development. Nat Rev Cancer. 2009; 9:537–549. [PubMed: 19629069]

Waldmeier P, Bozyczko-Coyne D, Williams M, Vaught JL. Recent clinical failures in Parkinson's disease with apoptosis inhibitors underline the need for a paradigm shift in drug discovery for neurodegenerative diseases. Biochem Pharmacol. 2006; 72:1197–1206. [PubMed: 16901468]

Wang X, Mader MM, Toth JE, Yu X, Jin N, Campbell RM, et al. Complete inhibition of anisomycin and UV radiation but not cytokine induced JNK and p38 activation by an aryl-substituted dihydropyrrolopyrazole quinoline and mixed lineage kinase 7 small interfering RNA. J Biol Chem. 2005; 280:19298–19305. [PubMed: 15737997]

Wang X, Chao L, Li X, Ma G, Chen L, Zang Y, et al. Elevated expression of phosphorylated c-Jun NH2-terminal kinase in basal-like and "triple-negative" breast cancers. Hum Pathol. 2010; 41:401–406. [PubMed: 19913278]

Wo JY, Chen K, Neville BA, Lin NU, Punglia RS. Effect of Very Small Tumor Size on Cancer-Specfic Mortality in Node-Positive Breast Cancer. Journal of Clinical Oncology. 2011

Yang Q, Deng X, Lu B, Cameron M, Fearns C, Patricelli MP, et al. Pharmacological inhibition of BMK1 suppresses tumor growth through promyelocytic leukemia protein. Cancer Cell. 2010; 18:258–267. [PubMed: 20832753]

Yu JL, May L, Lhotak V, Shahrzad S, Shirasawa S, Weitz JI, et al. Oncogenic events regulate tissue factor expression in colorectal cancer cells: implications for tumor progression and angiogenesis. Blood. 2005; 105:1734–1741. [PubMed: 15494427]

Zen K, Yasui K, Nakajima T, Zen Y, Gen Y, Mitsuyoshi H, et al. ERK5 is a target for gene amplification at 17p11 and promotes cell growth in hepatocellular carcinoma by regulating mitotic entry. Genes Chromosomes Cancer. 2009; 48:109–120. [PubMed: 18973138]

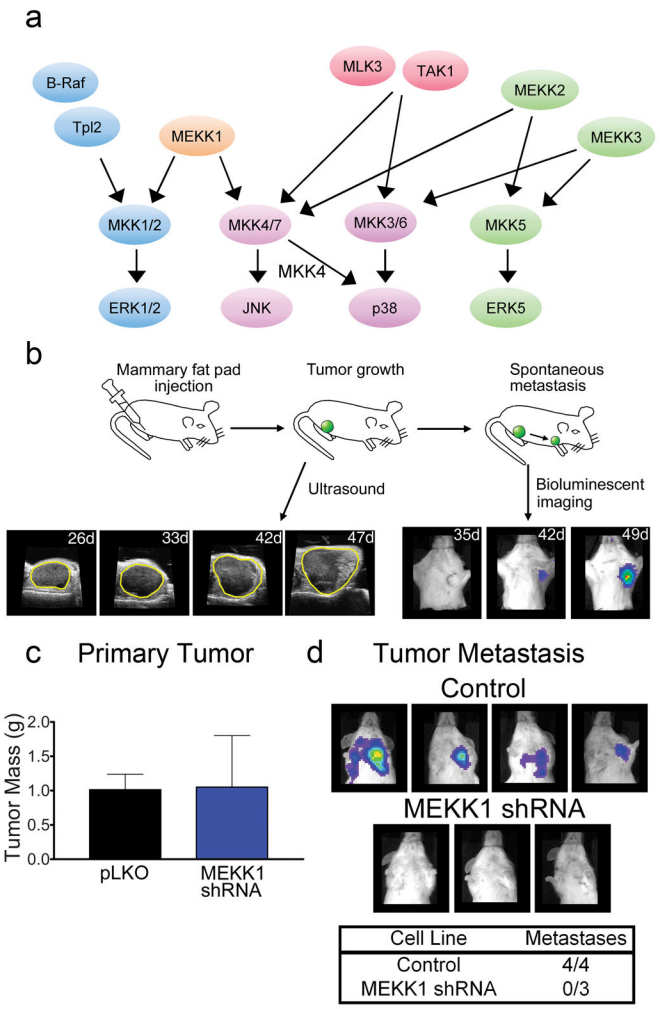

Figure 1.

Methods for the orthotopic xenograft assay used to define MAP3K control of tumor growth and metastasis. (a) MAPK network regulated by the seven MAP3Ks screened by stable shRNA knockdown in MDA-MB-231 cells. (b) Orthotopic mammary fat pad xenografts of control and MAP3K shRNA knockdown cells were used to assess specific MAP3K function in tumor growth and metastasis. Ultrasound was used to assess tumor volume and BLI was used to identify metastases. Ultrasound and BLI measurements were generally started at week 3 or 4 post injection and performed weekly until sacrifice of the animal. (c and d) As proof of concept, MEKK1 was shown to inhibit metastasis but not tumor growth. MEKK1 was previously shown in the PyMT mammary adenocarcinoma model to suppress metastasis but not tumor mass (Cuevas et al 2006). (c) Tumor mass (mean ± SEM) of control (n=4) and MEKK1 shRNA (n=3) MDA-MB-231 cells measured at 12 weeks post injection at time of sacrifice. (d) BLI for detection of metastases from tumors formed from control cells or MEKK1 shRNA cells measured at 12 weeks post injection at time of sacrifice.

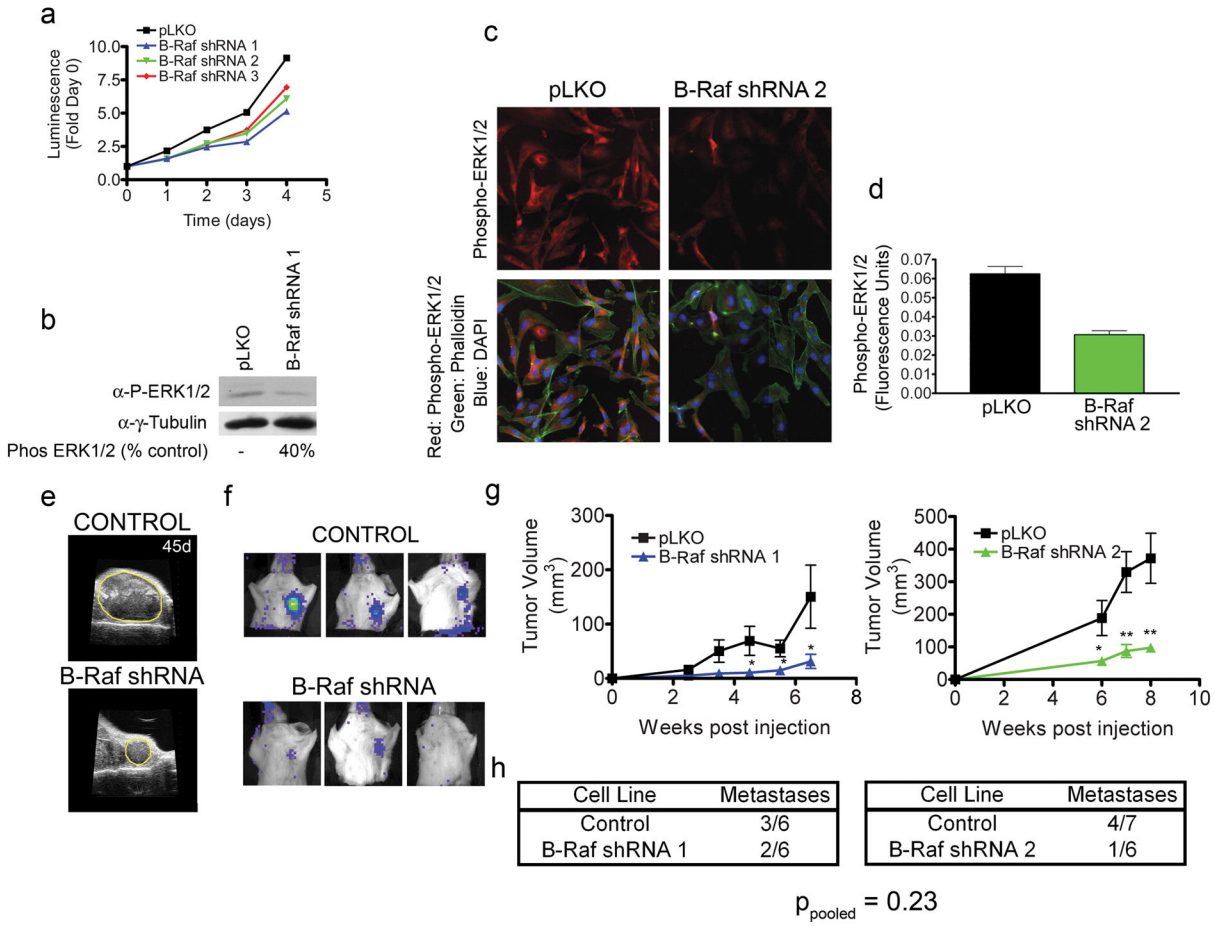

Figure 2.

ShRNA knockdown of B-Raf inhibits cell proliferation and xenograft tumor growth. (a) Three independent shRNAs were used for B-Raf knockdown in MDA-MB-231 cells. Control cells were selected with pLKO empty vector. The four lines were seeded at 10^5 cells per well and viability assessed in quadruplicate every 24 h for 4 days using Cell TiterGlo. (b) ERK1/2 activation is inhibited in B-Raf shRNA1 knockdown cells. Serum starved control and B-Raf shRNA cells were blotted for either phospho-ERK1/2 or gamma tubulin as a loading control. (c) Control and B-Raf shRNA2 cells have loss of phospho-ERK1/2 measured by immunoflourescence. Phospho-ERK1/2 (Red), actin (green) or nuclei (blue). (d) Quantitation of phospho-ERK1/2 immunostaining in control and B-Raf shRNA cells. Whole cells were masked using phalloidin-labeled actin. Phospho-ERK1/2 staining within the mask was quantitated for control and B-Raf shRNA cells. (e) Representative ultrasound images of control and B-Raf knockdown tumors at 45 days post injection. Outline of tumors is denoted with yellow line. (f) BLI of metastases from control and B-Raf tumors at 45 days for B-Raf shRNA1 (left panel) and 48 days for shRNA2 (right two panels showing one positive and one negative animal). (g) Quantitation of tumor volume in control and multiple B-Raf shRNA tumors. For each time point, data is presented as mean ± SEM, n = 6 (Control and B-Raf shRNA 1) and n = 7 (Control for B-Raf shRNA 2) or n = 6 (B-raf shRNA 2) * $p < 0.05$, ** $p < 0.01$ by unpaired t-test. (h) Number of mice metastasis positive at time of

sacrifice (day 55 post injection for control, shRNA1 & 2 mice). p-values for pooled control mice vs. pooled B-Raf shRNA mice were calculated by Fisher's exact test. Note: the control cohort for B-Raf shRNA 1 and TAK1 shRNA 1 are derived from the same experiment as they were done at the same time.

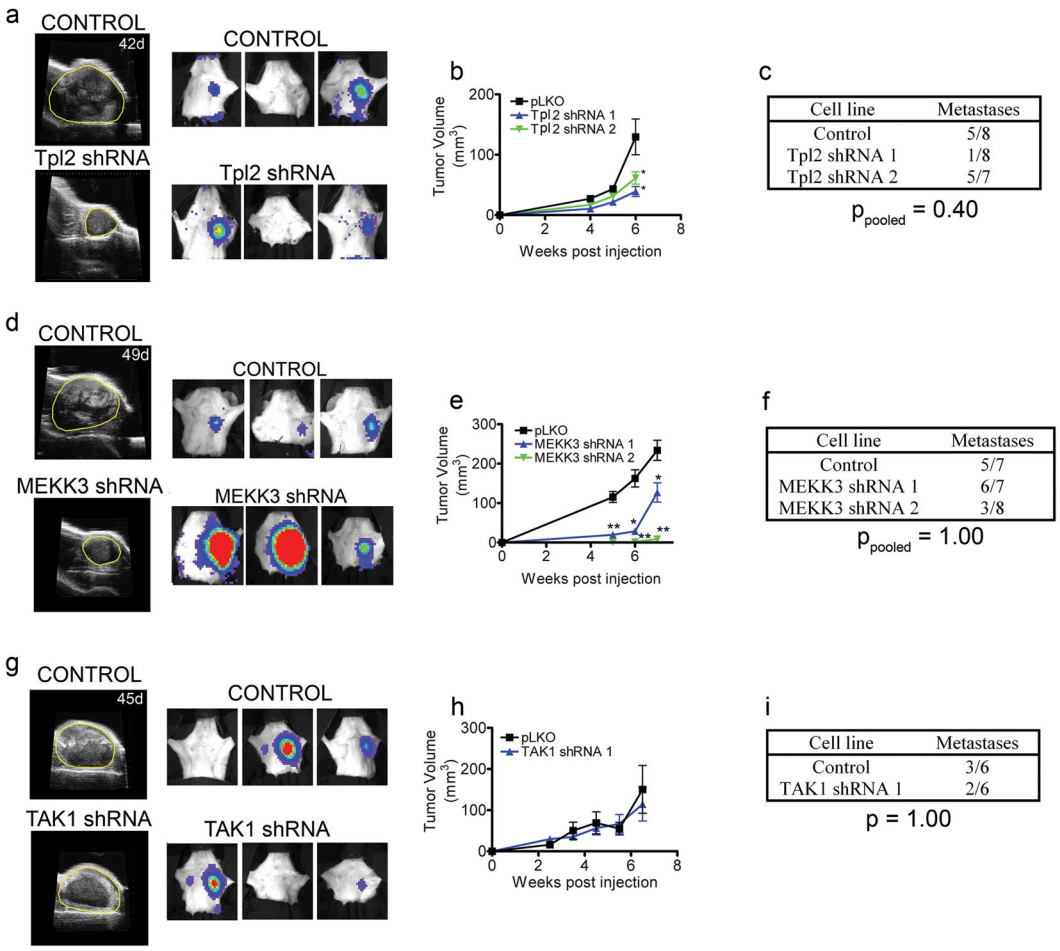

Figure 3.

Analysis of Tpl2, MEKK3 and TAK1 knockdown on tumor growth and metastasis. (a) Ultrasound and bioluminescent images of primary tumors and metastases for control and Tpl2 knockdown tumors. Tumor area is denoted with yellow line in ultrasound images. (b) Quantitation of tumor volume in control and Tpl2 knockdown cell lines demonstrating decreased tumor growth in two independent Tpl2 knockdown cell lines. For each time point, data is presented as mean ± SEM, n = 8 (Control and Tpl2 shRNA 1) or n = 7 (Tpl2 shRNA 2) * $p < 0.05$ by unpaired t-test. (c) Number of metastasis positive mice at time of sacrifice (57 days post injection) by BLI with control and Tpl2 knockdown tumors. p-values for pooled control mice vs. pooled Tpl2 shRNA mice were calculated by Fisher's exact test. (d) Ultrasound and BLI of primary tumors and metastases for control and MEKK3 knockdown tumors. Tumor area is denoted with yellow line in ultrasound images. (e) Quantitation of control and MEKK3 knockdown tumor volume determined by ultrasound imaging. For each point, data is presented as mean ± SEM for n = 7 (Control and MEKK3 shRNA 1) or n = 8 (MEKK3 shRNA 2) * $p < 0.05$, ** $p < 0.001$ by unpaired t-test. (f) Number of metastasis positive mice at time of sacrifice (57 days post injection). p-values for pooled control mice vs. pooled MEKK3 shRNA mice were calculated by Fisher's exact test. (g) Ultrasound images of primary tumors and BLI of metastases from tumors formed by injection of control and TAK1 shRNA containing cell lines. (h) Quantitation of tumor growth in control and

TAK1 shRNA tumors. For each time point, data is presented as mean ± SEM, n = 6 (Control and TAK1 shRNA 1) (i) Number of metastasis positive mice at time of sacrifice (55 days post injection for control and TAK1 shRNA 1. p-value for control mice vs. TAK1 shRNA 1 mice was calculated by Fisher's exact test. Note: the control cohort for B-Raf shRNA 1 and TAK1 shRNA 1 are derived from the same experiment.

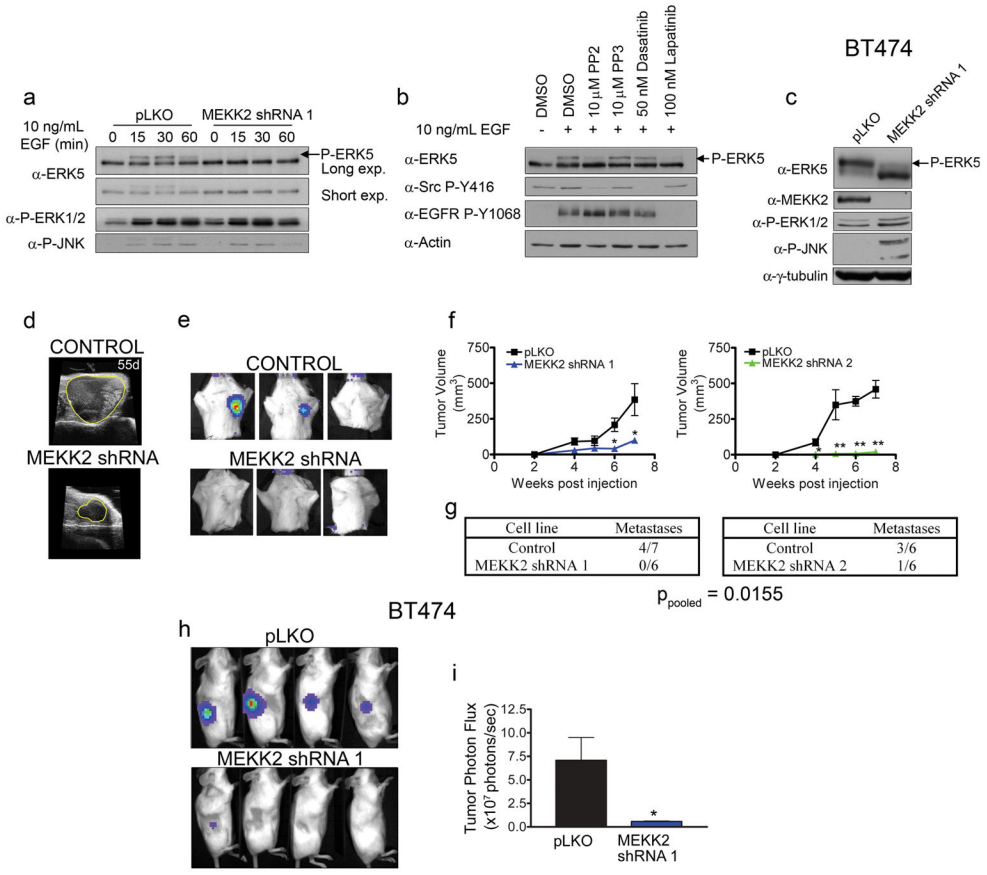

Figure 4.

MEKK2 mediates activation of ERK5 by EGFR and Her2 and is required for tumor growth and metastasis. (a) MEKK2 knockdown inhibits ERK5 activation in response to EGF. Cells were stimulated with 10 ng/mL EGF for the indicated times and blotted for ERK5, phospho-ERK1/2 and phospho-JNK. For ERK5 blots, long exposures were performed to identify the super-shifted phosphorylated form of ERK5 (arrows), while shorter exposures were performed to demonstrate equal loading of samples. (b) Requirement of EGFR and Src for ERK5 activation in MDA-MB-231 cells. Cells were serum starved and treated with DMSO control, PP2, PP3, Dasatinib or Lapatinib for 15 min prior to stimulation with 10 ng/mL EGF for 15 min. Cells were lysed and blotted for total ERK5, Src family Phospho-Y416, EGFR phospho-Y1068 or actin as a loading control. (c) Lysates from control and MEKK2 shRNA expressing BT474 cells were blotted for ERK5, MEKK2, phospho-ERK1/2, phospho-JNK or tubulin as a loading control. MEKK2 knockdown was accompanied by a marked loss of the super-shifted phospho-ERK5. (d) Ultrasound images of control and MEKK2 knockdown tumors 55 days post injection. (e) BLI detection of metastases in mice having control and MEKK2 knockdown tumors. (f) Quantitation of tumor volume in control and MEKK2 knockdown determined by ultrasound imaging (tumor area is denoted with yellow line). Each data point, data is presented as mean ± SEM for n = 7 and 6 (Control and MEKK2 shRNA 1) or n = 6 (Control and MEKK2 shRNA 2) * $p < 0.05$, ** $p < 0.002$ by unpaired t-test. (g) Number of metastasis positive mice at time of sacrifice (51 days post injection for control and shRNA 1 or 55 days post injection for control and shRNA 2. p-

values for pooled control mice vs. pooled MEKK2 shRNA mice were calculated by Fisher's exact test. (h) MEKK2 knockdown inhibits tumor growth of BT474 cells. BLI of flank tumors from mice injected with control or MEKK2 knockdown BT474 cells at 45 days post injection of cells. (i) Quantitation of tumor photon flux from control and MEKK2 shRNA BT474 tumors. Bars represent mean ± SEM for each cell type, n = 12 (control) n = 10 (MEKK2 shRNA 1), * $p < 0.05$ vs control.

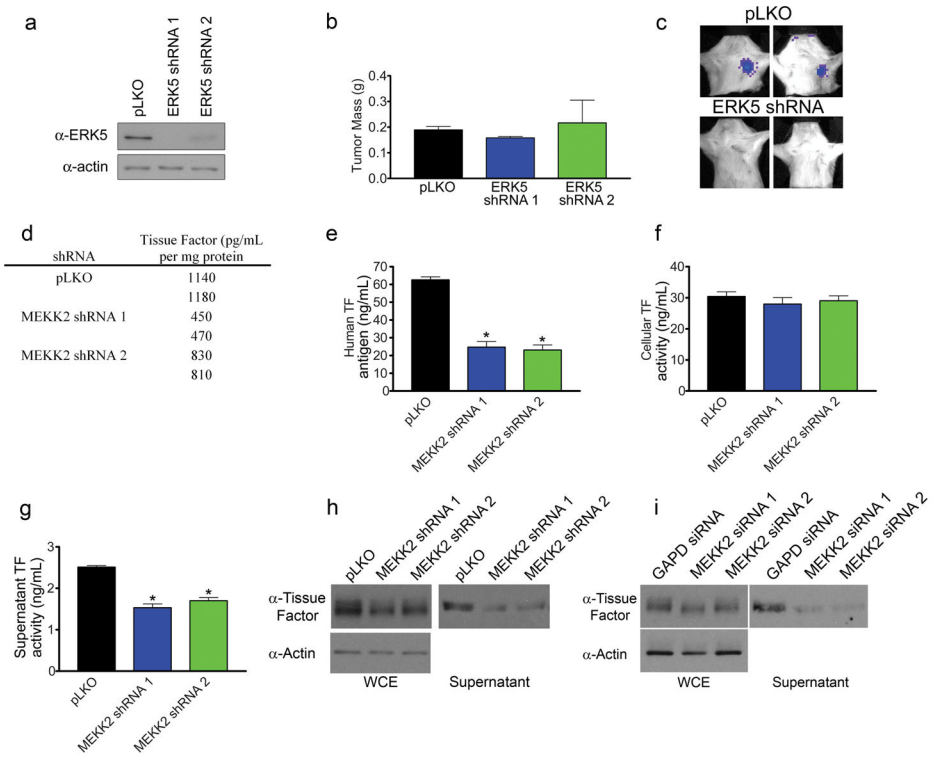

Figure 5.

ERK5 dependent metastasis and MEKK2 dependent release of TF+ microparticles (TF+ MPs). (a) Western blot analysis for ERK5 expression for control and ERK5 shRNA MDA-MB-231 cells. (b) Quantitation of tumor weight from mice injected with control and ERK5 shRNA cell lines. Bars represent mean ± SEM, n = 5 for each cell line. (c) BLI identifying metastases in control tumor mice but not in mice with ERK5 shRNA MDA-MB-231 cell tumors. One of 10 mice having ERK5 knockdown cell tumors developed a metastasis (d) Diminished TF from MEKK2 knockdown cells detected by multianalyte profiling of tissue culture supernatants. (e) ELISA detection of tissue factor in supernatants from control and MEKK2 knockdown cell lines. * $p < 0.001$ against control by t-test. (f) Cell associated TF activity in control and MEKK2 shRNA cell lines detected by chromogenic assay. (g) TF activity in purified microparticles isolated from control and MEKK2 shRNA cells. * $p < 0.001$ against control by t-test. (h,i) Western blots for TF from whole cell lysates and culture supernatants after RNAi knockdown of MEKK2. Supernatants were normalized to total cellular protein. (h) MEKK2 shRNA cell lines or (i) cells transfected with MEKK2 siRNAs. Representative of 3 independent experiments.

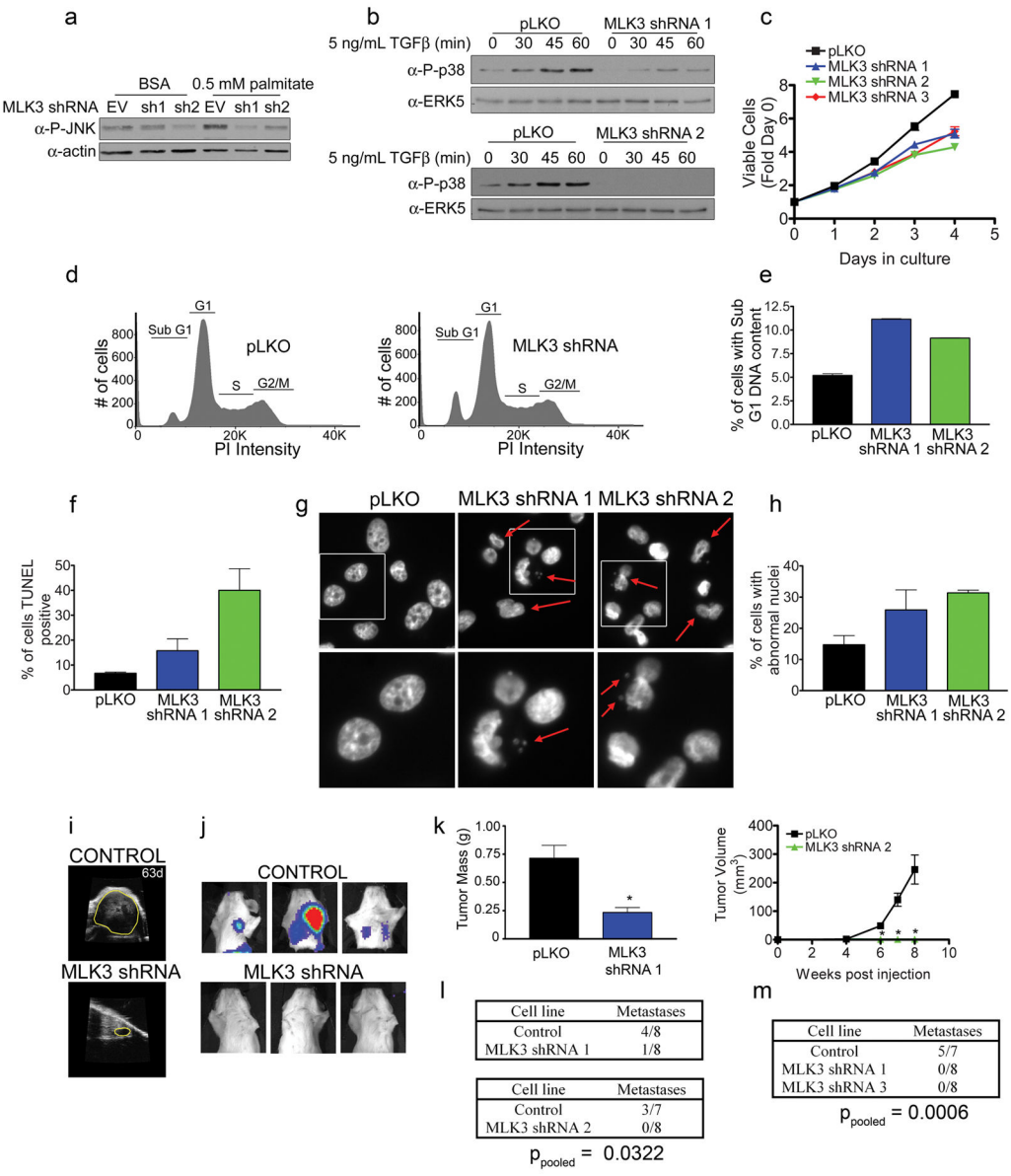

Figure 6.

Knockdown of MLK3 induces apoptosis and inhibits tumorigenesis. (a) MLK3 knockdown inhibits JNK activation by free fatty acid. Control, MLK3 shRNA 1 and MLK3 shRNA 2 cell lines were treated with either 0.5% fatty acid free BSA or 0.5 mM palmitate in 0.5% fatty acid free BSA for 18 hrs and lysates analyzed for phospho-JNK. (b) MLK3 knockdown inhibits TGFβ-stimulated p38 activation. Control and MLK3 shRNA 1 or control and MLK3 shRNA 2 cell lines were serum starved and treated with 5 ng/mL TGFβ for different times and analyzed for phospho-p38 or total ERK5 as a loading control. (c) Growth of control and MLK3 shRNA MDA-MB-231 cell lines over 4 days measured using the Cell TiterGlo viability assay. Individual measurements were normalized to day 0 signal. Each data point is the mean ± SEM of quadruplicate samples. (d) MLK3 knockdown increases the number of cells with sub G_0/G_1 DNA content. Representative FACS profiles are shown of propidium

iodide stained control and MLK3 knockdown MDA-MB-231 cells. (e) Quantitation of percentage of cells with sub G_0/G_1 DNA content detected by FACS in control and MLK3 knockdown cell lines. (f) Quantitation of TUNEL positive cells in control and MLK3 knockdown cell lines. Data are mean ± SEM for triplicate samples. (g) Control and MLK3 shRNA cells were stained with DAPI to visualize nuclear morphology. Top panels: Cells with aberrant nuclei are indicated with red arrows. Areas indicated in white boxes are enlarged in the bottom panels. Bottom panels: Red arrows indicate micronucleation within the MLK3 shRNA cells. (h) Quantitation of the percentage of cells with abnormal nuclei in control and MLK3 knockdown cell lines. For each condition ~200 cells were counted, n = 3. (i) Ultrasound images of control and MLK3 knockdown tumors 63 days post injection. Margins of tumor are indicated by yellow line. (j) BLI detection of metastases in mice having control and MLK3 knockdown tumors. (k) Quantitation of tumor size by tumor weight or tumor volume for control and MLK3 shRNAs. Each data point is mean ± SEM, n = 8 (control and MLK3 shRNA 1) or n = 7 and 8 (Control and MLK3 shRNA 2), * $p < 0.01$ by unpaired t-test. (l, m) Number of metastasis positive mice at time of sacrifice at 74 days (control and MLK3 shRNA 1), 73 days (control and MLK3 shRNA 2) or 51 days (control, MLK3 shRNA 1 and MLK3 shRNA 3). p-values for pooled control mice vs. pooled MLK3 shRNA mice were calculated by Fisher's exact test.